Journal of Molecular Modeling (2021) 27: 116
https://doi.org/10.1007/s00894-021-04725-0

ORIGINAL PAPER

A theoretical study to the loliolide molecule and its isomers: a study by circular dichroism, QTAIM, and NMR theoretical methods

Gunar Vingre da Silva Mota[1] · Fabio Luiz Paranhos Costa[2]

Received: 27 December 2020 / Accepted: 14 March 2021 / Published online: 31 March 2021

Abstract

The determination of an absolute configuration is a challenge in the structure elucidation of chiral natural products. With advancements in computational chemistry of chiroptical spectroscopy, the time-dependent density functional theory (TDDFT) calculation has emerged as a very promising tool. This paper attempts to illustrate the applicability of computational approaches in comparison with experimental data to understand the conformation, interaction, and stabilization of the loliolide's isomers. The quantum chemical calculations were used from optimized geometries of the (6R,7aS)-, (6S,7aR)-, (6R,7aR)-, and (6S,7aS)-6-hydroxy-4,4,7a-trimethyl-6,7-dihydro-5H-1-benzofuran-2-one. The spectroscopic values were obtained for ^{13}C NMR isotropic shielding by GIAO method in mPW1PW91/cc-pVTZ level, in TDDFT at the ωB97X-D/cc-pVTZ level to the circular dichroism, and in theoretical analyses of non-covalent interaction to study the isomer's stability. The TDDFT calculation of circular dichroism can be used to quantify the individual isomers and the nature of excitation in the molecule. The (6R,7aS) and (6R,7aR) isomers present a higher stability due to electronegativity associated at the hydroxyl group.

Keywords Electronic circular dichroism · Loliolide · Chemical shift · Non-covalent interaction · QTAIM

Introduction

In the chemistry of natural products, NMR spectroscopy is a very important tool, once it provides information about the planar configurations, conformations, and structure of natural products, due to parameters provided by NMR [1]. In many cases, the determination of the molecular conformation of a natural product can be terminated by the characterization of the correlation between H-H and H-C bonds. Although it is possible to determine the molecular structure, evaluations of the coupling constants and effects such as Overhauser (NOEs) provide information on the stereochemistry of compounds, with relative precision [2]. Stereochemical assignment can represent a challenge when the molecule has several degrees of freedom in its structure, making the analysis from the coupling constant and NOEs inconclusive [3].

Nowadays, the use of computational methods has become an important tool in the elucidation and characterization of molecules, especially, in the processes of prediction of chemical shifts. Concerning the assignment and reassignment of various natural products, it has been most frequent [4, 5]. Theoretical approaches used for the study of NMR spectra of organic molecules, mainly in the development of new protocols for signaling spectra from parameters such as ^{1}H and ^{13}C, have shown excellent results, even without taking into account the effects of interaction with the solvent, where we show that level of the theory requires less computational cost and the minimization of error in the chemical shifts, which is based on the linear regression between theoretical and experimental values, using TMS as a reference [6, 7].

An approach that has been used by our group successfully in the determining of the chemical shift (σ) is the use of GIAO-HDFT (hybrid density functional theory). We show that level of the theory requires a less computational cost, and the minimization of error in the precision of chemical shift is based on the linear regression between theoretical and

This paper belongs to the Topical Collection VIII Symposium on Electronic Structure and Molecular Dynamics – VIII SeedMol

✉ Gunar Vingre da Silva Mota
gunar@ufpa.br

[1] Natural Science Faculty, UFPA, ICEN, Belém, PA 66075-110, Brazil

[2] Department of Chemistry, UFJ, Jataí, GO 75801-615, Brazil

experimental values, using the TMS (tetramethylsilane) as reference. In our opinion, the first source of the problem in this method is due to the limited capacity of theoretical methods to determine a real molecular conformation, in some cases, which can influence the values of chemical shift. The second source of the problem is the impossibility of assignment of the correct conformation for the stereoisomers, being necessary the use of other methods (theoretical or experimental). A problem of determining only by chemical shifts is to identify which stereoisomer should be assigned.

The circular dichroism (CD) spectroscopy is widely used in the determination of secondary structures of organic molecules in solution (as in the case of proteins and peptides) [8, 9]. Each structure provides us a fingerprint, which has as a characteristic sequence of positive and negative peaks in the spectrum. This structural sensitivity results from dependence of the orientation of the electronic transitions. Generally, the CD spectra are described in terms of the rotational strength of electronic transitions, which depends on its dipole moments or its transition charge density, with respect to the electronic transitions between HOMO and LUMO [10, 11]. However, this characteristic will be found in any optically active molecule, due to their dextrorotary and levorotary components.

The quantum theory of atoms in molecules (QTAIM), developed by Richard F. W. Bader and his coworkers [12], depend on the position space in terms of the basins of the attractors (critical points). The connectivity of the critical points of the electron density gradient field provides information about its topology and of the molecular interactions. There are four types of critical points: nuclear attractor (NA), bond critical point (BCP), ring critical point (RCP), and cage critical point (CCP). This theory is a tool that can be used to elucidate the formation of stereoisomers for some molecules, which is based on the observation of electronic, topological density and displacement indices σ(H,H′) and proton-proton coupling constant [13–15]. This study will give us an idea about the interactions of hydrogens and their molecular stabilization. The electron density topology of various intramolecular and intermolecular interactions is a way to comprehend the strength of the interactions, and this way we can understand the nature interaction of bonds in accordance with the QTAIM hypotheses for the charge concentration ($\nabla^2\rho(x)$), kinetic energy density (G) e virial potential energy (V) for BCPs [16, 17].

The non-covalent interaction (NCI) [18, 19] method is used to identify and classify intermolecular and intramolecular interactions in small or large molecular systems. Due to the low computational costs, these methods are commonly used in all fields of chemistry, drug design [20], and large biological systems [21]. The NCI method, commonly referred to as an atomic interaction in line, can be observed in most cases where we would not expect a chemical interaction. The NCI method solves an associated problem at the QTAIM theory, in which the absence of an atomic interaction does not suggest that electron density cannot be concentrated in a region between atoms. These densities are then classified as destabilizing (when electron density is depleted) or stabilizing (when electron density is concentrated). Therefore, NCI calculations provide an identification of the interaction in three-dimensional space, show the electron density concentration, and can be used in a very large system. The nature of the energetic stabilization can explain controversial interactions in a molecular system, once that concentration regions are stabilized and attractive, and the depletion regions are often a steric strain [18, 19, 22–24].

In this work, our objectives are to investigate the stereochemistry of the loliolide molecule, due to the numbers of errors in the assignments of its isomers in the literature, and to gain a better understanding of transition evolving in the CD spectrum of each molecule. Figure 1 shows the molecular geometry to (6R,7aS), (6S,7aR), (6R,7aR), and (6S,7aS) isomers, which are commonly called (+)-loliolide, (−)-loliolide, epiloliolide, and isololiolide, respectively. The loliolide has great potential in the pharmaceutical industry, which can be used as a wound-healing, anti-inflammatory, and wrinkle-improving compound [25]. Their biological activity has action repellent, immunosuppressor, cytotoxic against nasopharyngeal carcinoma, lymphocytic leukemia, antioxidant mechanism, and protective capacity of cells against the apoptosis process [26, 27].

Few data are found in the literature on the isomers of loliolide, and works like that by Chen et al. [28] showed X-ray diffraction studies on the molecular structure of the loliolide using direct methods of analysis, which attributes their geometry of the (6R,7aS) isomer. Valdes [29] reported the NMR analysis, extraction, and isolation of the loliolide molecule from *Salvia divinorum* plants, which presents a conformational structure similar to the (6S, 7aR) isomer. Peng et al. [30] showed NMR analysis and isolation of the (6R,7aS) and (6S,7aS) isomers, obtained from Alga Sargassum naozhouense Tseng et Lu. Unfortunately, these isomers are in many cases being just called loliolide, and they usually are reported in the literature with a conformation molecular of the (6R,7aS) isomer.

The difficulties encountered to determine which isomer is being analyzed from NMR data lead us to compare different computational ways in comparison with experimental data to understand the formation of the isomers of a molecule, and the interaction related to molecular stabilization. In this way, we present some computational methods based on NMR experimental data found in the literature for the loliolide isomers and theoretical analyses of the isomer's stability concerning NCI and QTAIM theory.

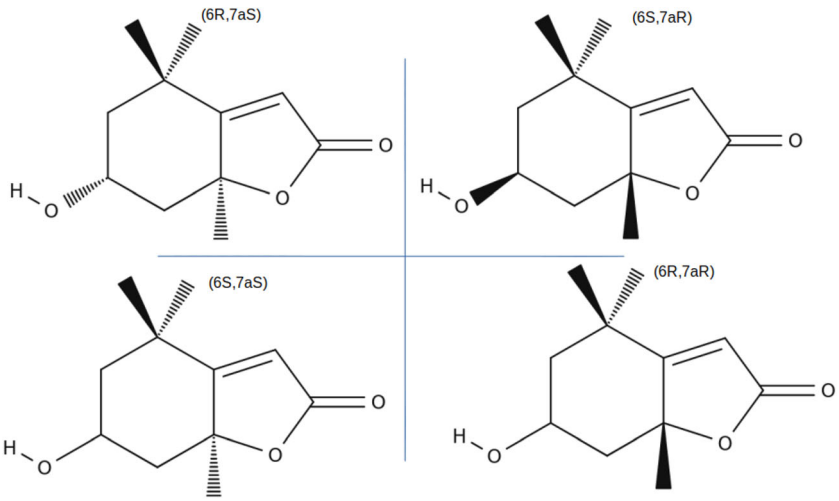

Fig. 1 Molecular geometry to (6R,7aS), (6S,7aR), (6R,7aR), and (6S,7aS) molecules. Where (6R,7aS) and (6S,7aR) isomers are commonly called (+)-loliolide and (−)-loliolide, respectively. The (6R,7aR) and (6S,7aS) isomers are commonly called epiloliolide and isoloiolide, respectively

Methods

The quantum chemical calculations were used to calculate the optimized geometries of the (6R,7aS), (6S,7aR), (6R,7aR), and (6S,7aS)-6-hydroxy-4,4,7a-trimethyl-6,7-dihydro-5H-1-benzofuran-2-one of the loliolide's isomers (Figure 1) by density functional theory method with the three-parameter hybrid functional (B3) for the exchange part, and the Lee-Yang-Par (LYP) correlation function at the 6-311G(d,p) basis set [31, 32]. All geometries correspond at the local minima in the potential energy surface (PES) in absence of imaginary frequencies.

Time-dependent density functional theory (TDDFT) at the ωB97X-D/cc-pVTZ level of theory was employed to calculate the excitation energy and rotatory strength $R_{0\lambda}$ (circular dichroism) for loliolide molecules. The choice of the ωB97X-D functional for our studies is due to contain an asymptotical portion of non-local exchange with dispersion corrections, which presents an accurate prediction in the process of charge-transfer excitation and hydrogen-bonding interactions [33].

Additionally, QTAIMs are performed and visualized using the AIMALL software [34]. We have selected two approaches: (1) QTAIM study for loliolide molecules and their isomers, and (2) the study of intramolecular non-covalent iterations (NCI). The NCI technique will be by the interpretation of the electronic density ($\rho(r)$) and its derivatives, called λ_2 eigenvalue in the Hessian matrix. The NCI calculation was carried out by the NCIplot software [35] and its isosurface was visualized in VMD [36].

The ^{13}C NMR isotropic shielding (σ) is calculated by the GIAO method [37] in mPW1PW91/cc-pVTZ level theory. The calculated chemical shift (δ_{calc}) was obtained by the differences between the isotropic shielding (σ) of each carbon nuclei in the target molecule with values to the isotropic shielding (σ) to the carbon nuclei obtained from tetramethylsilane (TMS, σ_{TMS}). The scaled chemical shift (δ_{scaled}) equation was obtained using the relationship between experimental (δ_{exp}) and computed (δ_{calc}) chemical shift. The equation to the scaling is of first degree of type: $\delta_{scaled} = a \times \delta_{cal} - b$, where a and b are the angular (slope of a line) and linear (vertical intercept) angular quantities in the Cartesian plane. The Gaussian 09 software program package [38] is used in all calculations in the ground (S_o) state.

Results and discussion

In this work, only the experimental values found in the literature for (6R,7aS) are presented, from X-ray crystallography carried out by Chen and collaborators [28]. Although we present only an experimental value for geometry, we can observe that the isomers can lead to erroneous measurements, for both computational and experimental measurements. A particularity concerning ^{13}C is related to the effect of the other nucleus which are minor on others, and coupling is not usually observed between carbons (J_{CC}), which occurs in around 1% of the carbons.

Figure 2 shows the calculations of the structural parameters of the stereoisomers (this work), which are close to the experimental values found by Chen and collaborators for (6R,7aS) isomer [28]. Therefore, the computational calculation might take to the result of the lowest energy isomer (in this work: 6R,7aS or 6S,7aR isomer), which might not correspond with the isomer studied.

As well as for other isomers, it is necessary to use more than one experimental and theoretical tools in the identification of stereoisomers for loliolide molecule, due to a slight difference in the molecular conformation. The results for the equilibrium conformations are shown in Table 1. The energy value is very close for the four isomers, due to similarity in the molecular conformations.

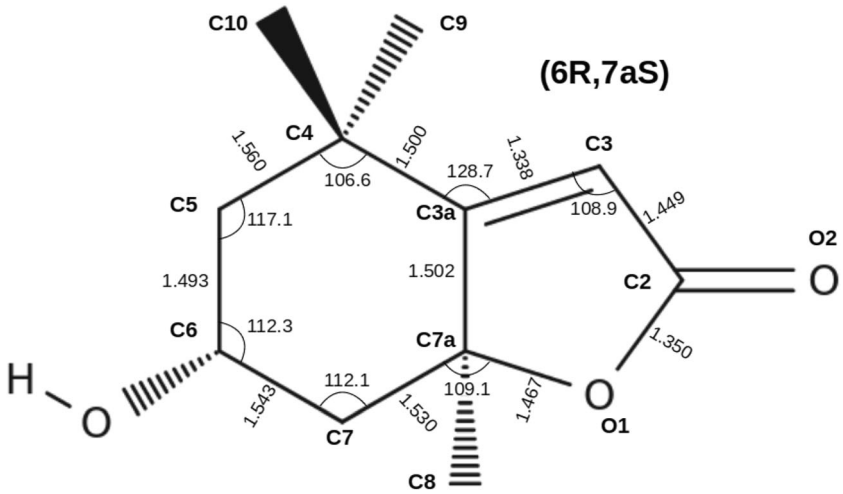

Fig. 2 Experimental values from X-ray crystallography to (6R,7aS)-6-hydroxy-4,4,7a-trimethyl-6,7-dihydro-5H-1-benzofuran-2-one [28]

Table 1 presents the values for experimental geometry, angles, and torsion for the (6R,7aS) molecule and the calculated value for the optimized structure. The average percentage error between these molecules is around 1.4%. Based

Table 1 Values for experimental geometry, angles, and torsion for the (6R,7aS) molecule and the calculated value for the optimized structure for (6R,7aS), (6S,7aR), (6R,7aR), and (6S,7aS) isomers

	Exp. [28]	Calculated			
	(6R,7aS)	(6R,7aS)	(6S,7aR)	(6R,7aR)	(6S,7aS)
Bond (å)					
r(O1-C2)	1.350	1.370	1.370	1.372	1.371
r(C2-C3)	1.449	1.462	1.462	1.462	1.463
r(C3-C3a)	1.338	1.335	1.335	1.334	1.334
r(C3a-C4)	1.500	1.488	1.488	1.490	1.490
r(C4-C5)	1.560	1.527	1.537	1.534	1.535
r(C5-C6)	1.493	1.515	1.515	1.513	1.512
r(C6-C7)	1.543	1.524	1.514	1.515	1.51
r(C7-C7a)	1.530	1.521	1.521	1.517	1.516
r(C3a-C7a)	1.502	1.501	1.501	1.502	1.503
r(C7a-O1)	1.467	1.436	1.463	1.434	1.434
Angle (°)					
a(C2-C3-C3a)	108.9	109.2	109.4	109.4	109.4
a(C3-C3a-C4)	128.7	129.8	129.1	129.3	129.3
a(C3a-C4-C5)	106.6	106.1	105.9	106.3	106.0
a(C4-C5-C6)	117.1	115.6	116.2	114.6	114.4
a(C5-C6-C7)	112.3	114.2	112.1	111.1	110.9
a(C6-C7-C7a)	112.1	112.6	113.0	111.1	110.9
a(C7-C7a-O1)	109.1	110.7	109.1	110.0	109.9
Torsion (°)					
t(O2-C2-C3-C3a)	−177.4	−178.7	−179.0	−179.2	−179.4
t(C2-C3-C3a-C4)	169.1	168.6	169.6	169.6	169.4
t(C3-C3a-C4-C5)	124.0	119.3	119.3	121.3	121.1
t(C3a-C4-C5-C6)	45.0	45.8	47.5	48.8	49.3
t(C4-C5-C6-C7)	−51.0	−51.8	−51.8	−56.9	−58.0
t(C5-C6-C7-C7a)	52.3	51.9	51.8	57.3	58.1
t(C6-C7-C7a-O1)	−162.4	−170.8	−162.7	165.7	165.8
Energy (eV)		−190.3072	−190.3071	−190.2990	−190.2866

on the experimental values, most of the geometric parameters are slightly larger; however, the connection length values for r(C4-C5) and r(C7a-O1) have a percentage error of around 2% smaller concerning the experimental values. For the angles, the average percentage error for the molecules concerning the experimental geometric value is around 1.5%, and for the average percentage error for (C3a-C4-C5) is ~2%, and for t(C3-C3a-C4-C5) and t(C6-C7-C7a-O1) is ~4% smaller and bigger, respectively.

When comparing the experimental geometry with the other isomers of loliolide, the similarity between the geometric parameters is clear. It can be observed for energy variation between (6R,7aS) and (6S,7aR) which is around 0.0001 eV, and between (6R,7aR) and (6S,7aS) is around 0.01 eV. Therefore, an optimization based on the planar geometrical (initial guess) may lead to the (6R,7aS) or (6S,7aR) isomer.

Table 1 shows the theoretical and experimental geometric parameters for the bonds, angles, and torsion angles. The experimental geometry values are only for (6R,7aS) molecules and the theoretical geometries show similarities between their isomers.

Geometry optimization calculations can cause errors in the spectroscopic properties of a molecule. A good example is the case of nuclear magnetic resonance spectroscopy, where theoretical calculations of NMR chemical shift depend on the molecular geometry. Thus, to minimize the error generated by geometry, it is necessary to use the scaling factor for the calculated chemical shift to have a smaller error concerning experimental values [39]. Although this process is to be practicable in many cases, it is still not enough to identify which isomer is studied.

Table 2 shows the results for the chemical shift of the experimental data of (6R,7aS), (6S,7aR), and (6R,7aR) found in the literature [29, 30]. Once the theoretical calculations were performed, a linear equation based on the relation between experimental and theoretical values of chemical shift is obtained. In this way, we seek to reduce the errors and improve accuracy for the theoretical values for the ^{13}C chemical shift. The linear equations obtained by the linear regression for each isomer are as follows: $\delta_{scaled}(6R,7aS) = 1.0081\delta_{cal} - 1.1163$, $\delta_{scaled}(6S,7aR) = 1.0031\delta_{cal} - 0.5843$, and $\delta_{scaled}(6R,7aR) = 1.0090\delta_{calc} - 1.1013$, where δ_{scaled} e δ_{cal} are the scaled and calculated values, respectively. We observed that calculations with B3LYP/c-pVTZ//B3LYP/6-311G(d) had shown that it is able to minimize errors in chemical shift, with a high correlation coefficient (R^2) and low computational cost.

The (6R,7aS) isomer showed a better correlation between experimental and theoretical data. However, it possible to observe a percent error of 5.76% for carbon C9 due to the difference between the C3a-C4-C5 angle, due to the non-planar conformation of the isomers. The same behavior happens to the (6R,7aS) isomer, because of the similarity between its conformations, which produces a percent error of 4.48% in the C9 carbon.

The linear regression is used frequently to correlate experimental and calculated values, mainly in NMR chemical shifts from the straight line which best represents the linear correlation between values. The result is subject to the uncertainty originated from basis sets, relativistic effects, and electronic correlation, which propagates to the values of magnetic shields [39].

A practice that is gaining popularity nowadays is the study of circular dichroism spectroscopy in the identification of isomers. The electronic circular dichroism (ECD) was performed for a range of 200-380 nm in this work (this choice is based on the effects of molecular chirality between the isomers). The rotational strengths in the ECD phenomenon are the signed numbers that represent the band intensities in the CD, in which the dipole strengths are associated with the CD absorption.

Table 2 Scaled values from B3LYP/c-pVTZ//B3LYP/6-311G(d) and experimental ^{13}C NMR chemical shifts (in ppm) in (6R,7aS), (6S,7aR), and (6R,7aR) isomers. All calculations are relative TMS solvent, using the same level of theory

	(6R,7aS)			(6S,7aR)			(6S,7aS)		
Carbon	Scaled	Exp. [30]	$\%_{error}$	Scaled	Exp. [29]	$\%_{error}$	Scaled	Exp. [30]	$\%_{error}$
C4	35.85	35.9	0.14	36.20	35.86	0.95	35.78	35	2.18
C7a	86.60	86.7	0.11	86.77	86.6	0.20	87.08	86.8	0.32
C3a	171.72	171.6	0.07	171.51	171.75	0.14	173.16	171.8	0.79
C5	46.15	45.7	0.98	44.33	45.75	3.20	46.04	47.8	3.83
C7	47.89	47.4	1.02	48.13	47.43	1.45	49.58	49.8	0.45
C6	67.47	66.8	0.99	67.61	66.84	1.14	63.71	64.6	1.40
C9	25.06	26.5	5.76	25.44	26.58	4.48	25.68	25	2.65
C10	26.98	27	0.07	27.71	27.03	2.47	26.29	25.4	3.39
C8	30.68	30.7	0.05	30.11	30.66	1.83	30.00	29.8	0.65
C3	113.55	112.9	0.57	114.45	112.97	1.29	112.12	112.9	0.69
C2	181.76	182.5	0.41	181.43	182.33	0.50	180.84	181.4	0.31

Unfortunately, the theoretical calculation of circular dichroism can only be associated with the corresponding band in the experimental spectra, due to experimental bands that cannot predict the cases of multiple transition overlap. Therefore, the simulated spectrum provides a good indication of positive and negative intensities in the identity of the bands.

Table 3 presents the values of electronic circular dichroism for a range from 200 to 300 nm for the loliolide isomers. The ECD values show negative and positive band intensities, indicated by rotational strengths, as well as the oscillator strengths and the nature of excitation. For the isomer (6R,7aS), the spectrum shows a positive maximum around 209 nm with a transition of type n → π*, originated from C=O → C=C transition and a negative maximum around 203 nm with a transition of type n → 1d Rydberg, originated from C=O → O-H transition. For the isomer (6S,7aR), the spectrum shows a positive maximum around 213 nm with a transition of type n → π*, originating from C-C → C=C transition, and a negative maximum around 210 nm with a transition of type π → π* and n → π*, originated from C=C → C=C and C=C → C=O transitions, respectively.

In the (6S,7aR) isomer, the predominant excitation nature is of the type π → π* and n → π* originated from carbon with sp^2 hybridization, while in all other isomers, we find at least one transition to a Rydberg orbital. The rotatory strength of (6R,7aR) is relatively weak, and the negative maximum intensity is redshifted concerning (6S,7aS) isomer. The rotatory strength of (6R,7aS) is relatively closed, and the negative maximum intensity is slightly redshifted concerning (6S,7aR) isomer.

Uchida and Kuriyama [40] showed a negative maximum at 219 nm as being a transition of the type π → π* (predominant), and a positive maximum at 268 nm with transitions of the type n → π*, in methanol. The theoretical value found was 218.2 and 287.5 nm, with the transition of the type π → π* and n → π*, respectively. The theoretical positive maximum is redshifted concerning the corresponding experimental absorption band, due to the absence of the solvent. However, the result shows an excellent agreement with the experimental results. Here, the theoretical results for the (6S,7aR), (6R,7aR), and (6S,7aS) isomers to understand the nature of the excitation of each one are presented (shown in Table 3).

Table 3 Molecular structures corresponding to the loliolide's isomers, positive and negative bands, oscillator strength (Osc.), and rotatory strength, R, in 10^{-40} cgs units

	Rotatory strength			
	Length/10^{-40} cgs	Velocity/10^{-40} cgs	Osc (a.u.)	Nature of excitation
(6R,7aS)*				
203.6	−43.529	−35.139	0.063260	n→1 s Rydberg
209.3	104.19	90.539	0.055416	n→π*
218.2	−33.811	−29.674	0.014282	π→π*; n→π*
233.3	−11.681	−7.4713	0.031266	π→π*
287.5	10.156	8.2269	0.000864	n→π*
(6S,7aR)				
210.2	−104.16	−101.82	0.109530	π→π*; n→π*
213.2	92.433	90.916	0.062993	n→π*
235.0	12.143	12.007	0.057414	π→π*
272.4	−11.374	−11.175	0.009207	π→π*
(6R,7aR)				
205.2	19.965	19.988	0.143660	π→1 s Rydberg
210.4	6.013	5.747	0.023190	π→π*
219.6	4.6926	3.9231	0.006173	π→1 s Rydberg, n→π*
237.1	−24.008	−23.654	0.053208	π→π*
(6S,7aS)				
204.2	54.197	53.336	0.047125	n→π*
208.8	24.515	27.072	0.017108	n→2 s Rydberg
211.7	−109.07	−112.31	0.158240	π→π*; n→π*
219.4	77.501	74.912	0.034390	n→π*
226.7	−6.3642	−6.7859	0.004224	n→2 s Rydberg
238.6	2.7257	3.414	0.038495	π→π*

Experimental values [40]: 219 nm (π → π transition); 268 nm (n → π* transition), in methanol

To understand the stability of isomers, we will study the inter-atomic interactions in each molecule from the theory of atoms and molecules. The use of theoretical calculations allows the determination of the probability to find an electron in a given volume of space, which is called the probability density distribution, and it is defined as a scalar field. When the probability density takes into account all the electrons in the molecule, it becomes known as an electron density distribution (or simply electron density) and is given by $\rho(x,y,z)$. The key to the bonding and geometry of a molecule is the electron density, due to forces that is holding the nuclei together being attractive between the electrons and the nuclei. It can be understood as the sum of the Coulombic forces exerted by the nuclei, and by the electron density distribution (ρ) [41]. The topology of the electron density of intramolecular and intermolecular interactions is an interesting methodology to evaluate the strength of interactions. The topological parameters of the type different of critical points (CPs) are the electron density ($\rho(r)$), the Laplacian of electron density ($\nabla^2\rho(r)$), the potential electron density ($V(r)$), and the Lagrangian kinetic electron density ($G(r)$), which has been analyzed by Bader's theory [12].

Figure 3 shows the contour map of the Laplacian of the electron density, $\nabla^2\rho$, for (6R,7aS), (6S,7aR), (6R,7aR), and (6S,7aS) isomers calculated by mPW1PW91/cc-pVTZ functional since the Dunning's correlation for this triple zeta basis set increases computational efficiency and its converge is smooth.

It is possible to observe by Figure 3 that the electron density for the isomers is very similar, and with a spherical shape around each nucleus. However, the (6S,7aS) isomer shows a charge distribution with a lower concentration in the H-O bond concerning the (6R,7aR) isomer. In these two isomers, there is the formation of only one BCP with values of $\rho =$ 0.014 a.u. and $\nabla^2\rho = 0.042$ a.u. between two hydrogens (H H), and one point RCP with values of $\rho = 0.008$ a.u. and $\nabla^2\rho = 0.026$ a.u. formed by the interaction of three hydrogens (dotted line).

This configuration provides stability to the isomers from the attractive steric interaction due to the non-covalent interactions, and since the interactions between the two hydrogens (H H) are weak, it provides stability for the formation of the conformer [22]. These conformations are associated with the presence of an intramolecular interaction between three hydrogens (indicated in Figure 3), which has a directional action and a steric formation induced by the appearance of a ring critical point (RCP) between these hydrogens. The charge distribution for the isomers (6R,7aS) and (6S,7aR) shows similarity in their densities; in other words, the nuclear regions do not show significant topological characteristics. The difference between the electron densities between the two isomers is only observed by their 3D isoforms, due to their chirality in their enantiomers, and the values of BCP and RCP have densities and concentrations higher than for the (6R, 7aR) and (6S,7aS) isomers. The conformations are associated with the presence of an intramolecular interaction between hydrogen and oxygen (indicated in Figure 4), which also has a directional nature of the action, and a steric formation induced by arising from the bond critical point (BCP) between these interactions.

From the non-covalent interaction (NCI) view, there is an important information about the covalent bonds between different functional groups within a single molecule [22]. It provides a representation of hydrogen bonds, van der Waals interactions, and steric repulsion in molecules. In the case of loliolide isomers, the difference between diastereomeric interacting pairs is based on the delicate interactions of H H interactions (triangular interaction between hydrogens), which is much weaker than the OH H interaction (triangular interaction between hydroxyl and hydrogens).

Figure 4 shows the (6R,7aS) and (6R,7aR) molecules and their characteristic non-covalent interactions. Due to optical isomerism, the behaviors of intramolecular interactions are similar in (6S,7aR) and (6S,7aS). In a system with intra and/or intermolecular interactions, it is possible to find the weak interactions associated with the van der Waals (vdW) and hydrogen bond (HB) interactions, which are the most common in non-covalent interactions.

Electronic density for interactions HO H ($\nabla^2\rho = 0.049$ a.u. and $\nabla^2\rho = 0.058$ a.u.) presents a concentration of greater than the interactions H · · · H ($\nabla^2\rho =$ 0.043 a.u. and $\nabla^2\rho =$ 0.044 a.u.) in both isomers. This difference is associated with the electronegativity of oxygen in the molecules. The higher charge concentration in RCP ($\nabla^2\rho =$ 0.034 a.u.) in the (6R,7aR) and (6S,7aS) isomers is due to the formation of weak directional interactions produced by BCPs, providing lower stability for the isomers. Conventionally, the hydrogen bonds are described in terms of the intermolecular interactions from medium to large strength, but the weaker strength in the intramolecular hydrogen bonds has an important function for molecular stabilization [42].

From the QTAIM result, which provides information about the repulsive (unfavorable) and attractive (favorable) interactions, the information of the strength of the interaction sign of the λ_2 eigenvalue is used. Depending on the interaction type, λ_2 can be either negative or positive, like in the cases of HB with $\lambda_2 < 0$ (accumulation of density perpendicular to the bond), SC with $\lambda_2 > 0$ (repulsion interaction), and vdW with $\lambda_2 \lesssim 0$ (negligible density overlap).

For the (6R,7aS) molecule, it is possible to observe an attractive van der Waals force interaction between HO H (largest region of interaction), and between H_3C HC (smallest region of interaction), which is a delocalized interaction due to accumulation of density which is closed due to molecular conformation; the same behavior will be found in all isomers. For the (6R,7aR) molecule, it is possible to

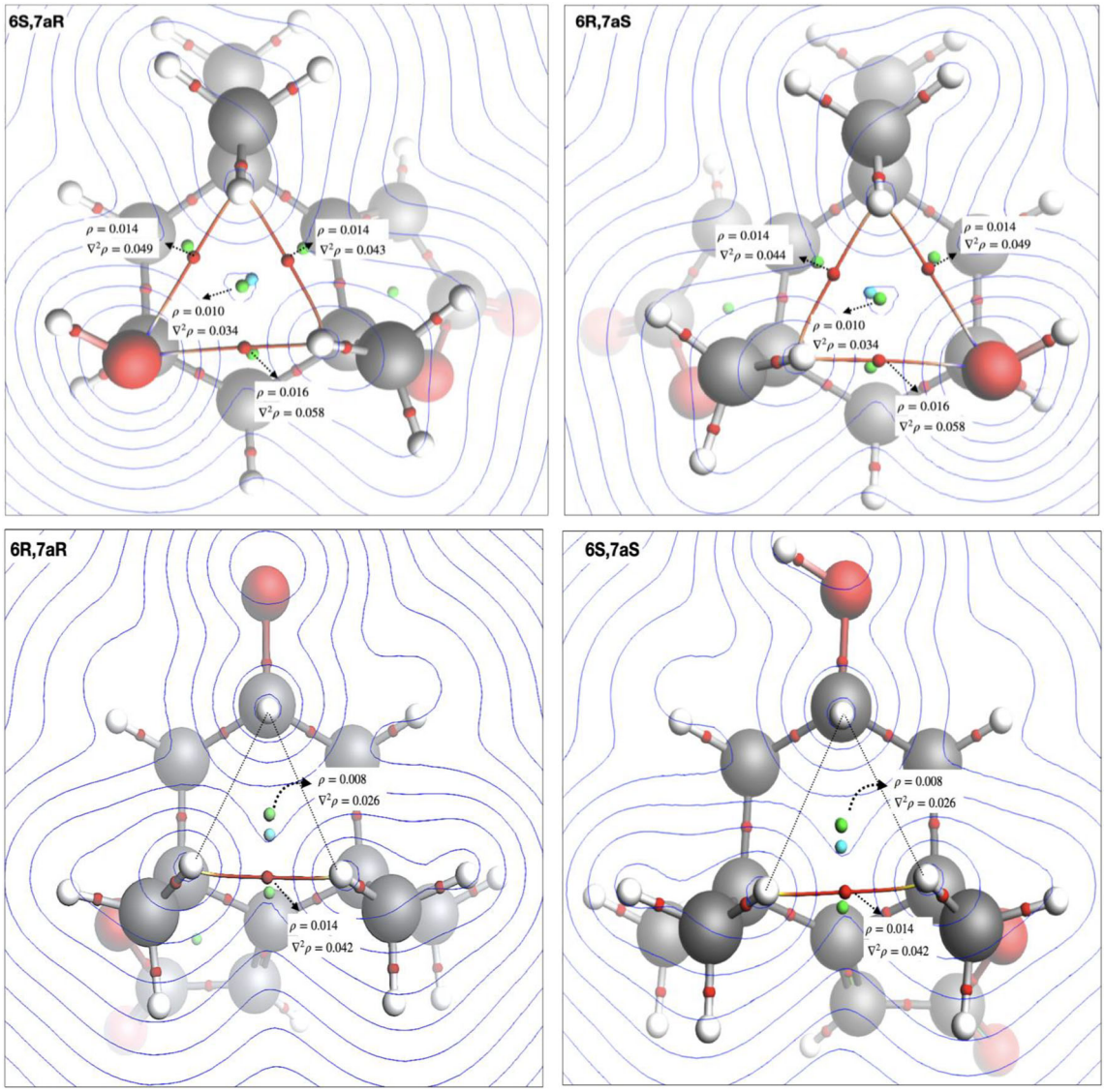

Fig. 3 Attractive steric interactions for the (6R,7aS), (6S,7aR), (6R,7aR), and (6S,7aS) isomers calculated by mPW1PW91/cc-pVTZ functional, and analyzed from Bader's theory [12]

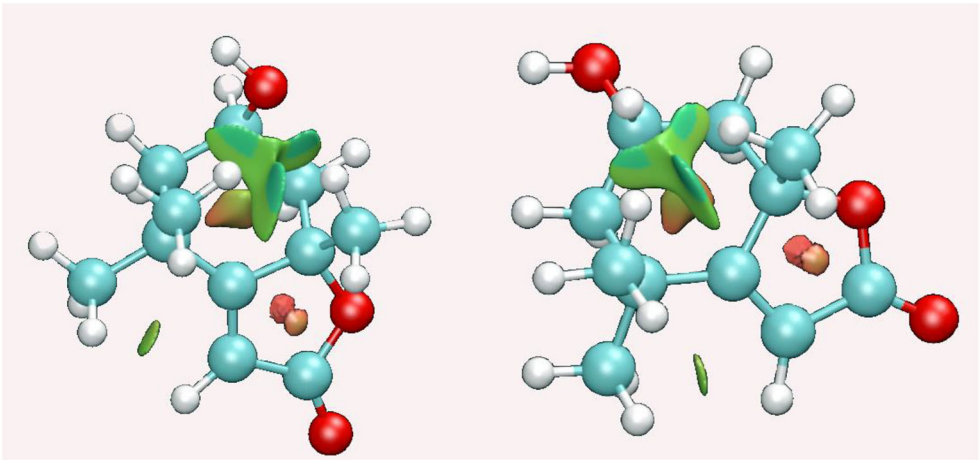

Fig. 4 Isosurface obtained by NCI calculation for (6R,7aS) e (6R,7aR) molecule. The same behavior will be found in the other isomers. The weak interactions are represented by the green colors

observe an attractive interaction of the type of hydrogen bond forces (greater region of interaction), where each atom-atom contribution is weak and it produces a decrease in the total electronic energy concerning the (6R,7aS) molecule. Repulsive interactions can be seen in red color, which represents a steric repulsion due to density depletion, which is illustrated by the density overlap in the central part of the ring. It is due to the sum of contributions from nearby atoms, and it is associated with a positive value of λ_2. These weak interactions are expected due to their lower critical electron densities (Figure 4). In general, the NCI procedure can describe the intramolecular interactions with base in the stabilizing and destabilizing components, which is depending on the strength of the interaction as well as on the ring length.

Conclusions

The computational methods, as TDDFT calculation, are a promising tool for the determination of structures of isomers of the organic molecules. Circular dichroism contains information about conformations and exhibited well-resolved bands of four isomers, as well as of the orientation relative to each other. QTAIM and NCI techniques were investigated to elucidate the molecular interaction governing the stable conformations. Attractive van der Waals force interaction between HO H are responsible by stabilization molecular, due to electronegativity of the hydroxyl group. NMR in principle did not differ the conformation molecular just by chemical shift. To determine an absolute conformation is necessary the combined theoretical investigation provides significant insights to understand the conformational structure as well as nature of the iterations on the isomers.

Supplementary Information The online version contains supplementary material available at https://doi.org/10.1007/s00894-021-04725-0.

Acknowledgements This work was partially supported by the Federal University of Pará.

Author contribution Gunar VS Mota devised the project, the main conceptual ideas, and the proof outline, and with help from Fabio LP Costa, we verified the numerical results of the chemical shift.

Fabio LP Costa performed the calculations of ^{13}C NMR, and Gunar VS Mota performed the calculations of circular dichroism, topological analysis, and other quantum calculations.

Both authors Gunar VS Mota and Fabio LP Costa contributed to the final version of the manuscript.

Availability of data and material N/A.

Code availability N/A.

Declarations

Ethics approval N/A.

Consent to participate N/A.

Consent for publication N/A.

Conflict of interest The authors declare no competing interests.

References

1. Kwan EE, Huang SG (2008) Structural elucidation with NMR spectroscopy: practical strategies for organic chemists. Eur J Org Chem:2671–2688
2. Matsumori N, Murata M (2017) NMR studies on natural product-stereochemical determination and conformational analysis in solution and in membrane. In: Experimental Approaches of NMR Spectroscopy: Methodology and Application to Life Science and Materials Science. pp 383–414
3. Smith SG, Goodman JM (2009) Assigning the stereochemistry of pairs of diastereoisomers using GIAO NMR shift calculation. J Organomet Chem 74:4597–4607. https://doi.org/10.1021/jo900408d
4. Neves Cruz J, Santana De Oliveira M, Gomes Silva S et al (2020) Insight into the interaction mechanism of nicotine, NNK, and NNN with cytochrome P450 2A13 based on molecular dynamics simulation. J Chem Inf Model 60:766–776. https://doi.org/10.1021/acs.jcim.9b00741
5. Lauro G, Das P, Riccio R et al (2020) DFT/NMR approach for the configuration assignment of groups of stereoisomers by the combination and comparison of experimental and predicted sets of data. J Organomet Chem 85:3297–3306. https://doi.org/10.1021/acs.joc.9b03129
6. Giacomello TF, Mota GV d S, Neto AM dJC, Costa FLP (2020) Use of replaced chalcones to generate a 13 C chemical shift staging factor for chalcone and its derivate. Adv Sci Eng Med 12:464–472. https://doi.org/10.1166/asem.2020.2548
7. Souza SS, Martins MA d S, Neto AM d JC et al (2020) Systematic gauge-including atomic orbital-hybrid density functional theory linear regressions for 13 C NMR chemical shifts calculation. Adv Sci Eng Med 12:364–370. https://doi.org/10.1166/asem.2020.2508
8. Woody RW (1992) Circular dichroism of unordered polypeptides. Adv Biophys Chem 2:37–79
9. Sreerama N, Woody RW (2000) Estimation of protein secondary structure from circular dichroism spectra: comparison of CONTIN, SELCON, and CDSSTR methods with an expanded reference set. Anal Biochem 287:252–260. https://doi.org/10.1006/abio.2000.4880
10. Woody RW (2009) Circular dichroism spectrum of peptides in the poly(Pro)II conformation. J Am Chem Soc 131:8234–8245. https://doi.org/10.1021/ja901218m
11. Moffitt W (1956) Optical rotatory dispersion of helical polymers. J Chem Phys 25:467–478. https://doi.org/10.1063/1.1742946
12. Orville-Thomas WJ (1996) Atoms in molecules—a quantum theory. Clarendon Press
13. Matta CF, Hernández-Trujillo J, Bader RFW (2002) Proton spin-spin coupling and electron delocalization. J Phys Chem A 106:7369–7375. https://doi.org/10.1021/jp020514f
14. Sánchez-Mendoza E, Hernández-Trujillo J (2010) Interpretation of vicinal proton-proton coupling constants of heteroaromatic

molecules in terms of topological electron density descriptors. Magn Reson Chem 48:866–872. https://doi.org/10.1002/mrc.2679
15. Mandado M, Blockhuys F, Van Alsenoy C (2006) On the applicability of QTAIM, Hirshfeld and Mulliken delocalisation indices as a measure of proton spin-spin coupling in aromatic compounds. Chem Phys Lett 430:454–458. https://doi.org/10.1016/j.cplett.2006.09.037
16. Lepetit C, Fau P, Fajerwerg K et al (2017) Topological analysis of the metal-metal bond: a tutorial review. Coord Chem Rev 345:150–181
17. Espinosa E, Molins E, Lecomte C (1998) Hydrogen bond strengths revealed by topological analyses of experimentally observed electron densities. Chem Phys Lett 285:170–173. https://doi.org/10.1016/S0009-2614(98)00036-0
18. Johnson ER, Keinan S, Mori-Sánchez P et al (2010) Revealing noncovalent interactions. J Am Chem Soc 132:6498–6506. https://doi.org/10.1021/ja100936w
19. Gillet N, Chaudret R, Contreras-García J et al (2012) Coupling quantum interpretative techniques: another look at chemical mechanisms in organic reactions. J Chem Theory Comput 8:3993–3997. https://doi.org/10.1021/ct300234g
20. Sukumar N, Breneman CM (2007) QTAIM in drug discovery and protein modeling. In: The Quantum Theory of Atoms in Molecules: From Solid State to DNA and Drug Design, pp 471–498
21. Churchill CDM, Rutledge LR, Wetmore SD (2010) Effects of the biological backbone on stacking interactions at DNA-protein interfaces: the interplay between the backbone···π and π···π components. Phys Chem Chem Phys 12:14515–14526. https://doi.org/10.1039/c0cp00550a
22. Chaudret R, De Courcy B, Contreras-García J et al (2014) Unraveling non-covalent interactions within flexible biomolecules: from electron density topology to gas phase spectroscopy. Phys Chem Chem Phys 16:9876–9891. https://doi.org/10.1039/c3cp52774c
23. Armstrong A, Boto RA, Dingwall P et al (2014) The Houk-list transition states for organocatalytic mechanisms revisited. Chem Sci 5:2057–2071. https://doi.org/10.1039/c3sc53416b
24. Otero-De-La-Roza A, Johnson ER, Contreras-García J (2012) Revealing non-covalent interactions in solids: NCI plots revisited. Phys Chem Chem Phys 14:12165–12172. https://doi.org/10.1039/c2cp41395g
25. Park SH, Kim DS, Kim S et al (2019) Loliolide presents antiapoptosis and antiscratching effects in human keratinocytes. https://doi.org/10.3390/ijms20030651
26. Borkosky S, Valdés DA, Bardón A et al (1996) Sesquiterpene lactones and other constituents of Eirmocephala megaphylla and Cyrtocymura cincta. Phytochemistry 42:1637–1639. https://doi.org/10.1016/0031-9422(96)82943-8
27. Okada N, Shirata K, Niwano M et al (1994) Immunosuppressive activity of a monoterpene from Eucommia ulmoides. Phytochemistry 37:281–282. https://doi.org/10.1016/0031-9422(94)85042-9
28. Chen JY, Chen JM, Xiao PG et al (1997) Crystal structure of loliolide (5,6,7a-tetrahydro-6-hydroxy-4,4,7a-trimethyl-2(4H)-benzofuranones). Jiegou Huaxue 16:335–337
29. Valdes LJ (1986) Loliolide from salvia divinorum. J Nat Prod 49:171. https://doi.org/10.1021/np50043a031
30. Peng Y, Huang RM, Lin XP, Liu YH (2018) Norisoprenoids from the Brown alga Sargassum naozhouense Tseng et Lu. Molecules 23. https://doi.org/10.3390/molecules23020348
31. Becke AD (1988) Density-functional exchange-energy approximation with correct asymptotic behavior. Phys Rev A 38:3098–3100. https://doi.org/10.1103/PhysRevA.38.3098
32. Becke AD (1993) Density-functional thermochemistry. III. The role of exact exchange. J Chem Phys 98:5648–5652. https://doi.org/10.1063/1.464913
33. Ilawe NV, Schweitzer-Stenner R, Diguiseppi D, Wong BM (2018) Is a cross-β-sheet structure of low molecular weight peptides necessary for the formation of fibrils and peptide hydrogels? Phys Chem Chem Phys 20:18158–18168. https://doi.org/10.1039/c8cp00691a
34. Keith TA (2017) AIMALL (Version 14.11.23),. TK Gristmill Software, Overl. Park KS, USA
35. Contreras-García J, Johnson ER, Keinan S et al (2011) NCIPLOT: a program for plotting noncovalent interaction regions. J Chem Theory Comput 7:625–632. https://doi.org/10.1021/ct100641a
36. Humphrey W, Dalke A, Schulten K (1996) VMD: visual molecular dynamics. J Mol Graph 14:33–38. https://doi.org/10.1016/0263-7855(96)00018-5
37. O'Boyle NM, Tenderholt AL, Langner KM (2008) Cclib: a library for package-independent computational chemistry algorithms. J Comput Chem 29:839–845. https://doi.org/10.1002/jcc.20823
38. Frisch MJ, Trucks GW, Schlegel HB, et al (2016) Gaussian09 revision D.01, Gaussian Inc. Wallingford CT. Gaussian 09 Revis. C.01 Gaussian Inc., Wallingford CT
39. Neto AMJC, Costa FLP, Mota GVS (2017) Minimization of the residual error as an alternative method for 13C chemical shift calculation. J Comput Theor Nanosci 14:2422–2428. https://doi.org/10.1166/jctn.2017.6843
40. Uchida I, Kuriyama K (1974) The π-π circular dichroism of δβ-unsaturated γ-lactones. Tetrahedron Lett 15:3761–3764. https://doi.org/10.1016/S0040-4039(01)92002-7
41. Rabinovich D (2003) Chemical bonding and molecular geometry: from Lewis to electron densities (Gillespie, Ronald J.; Popelier, Paul L. A.). J Chem Educ 80:31. https://doi.org/10.1021/ed080p31
42. Desiraju GR, Steiner T (1999) The weak hydrogen bond in structural chemistry and biology (International Union of Crystallography, Monographs on Crystallography, 9)